THE JOURNAL OF PHYSICAL CHEMISTRY B

ARTICLE

pubs.acs.org/JPCB

Convergent Raman Features in High Density Amorphous Ice, Ice VII, and Ice VIII under Pressure

Yukihiro Yoshimura,*[,†] Sarah T. Stewart,[‡] Maddury Somayazulu,[§] Ho Kwang Mao,[§] and Russell J. Hemley[§]

[†]Department of Applied Chemistry, National Defense Academy, 1-10-20 Hashirimizu, Yokosuka, Kanagawa 239-8686, Japan

[‡]Department of Earth and Planetary Sciences, Harvard University, 20 Oxford Street, Cambridge, Massachusetts 02138, United States

[§]Geophysical Laboratory, Carnegie Institution of Washington, 5251 Broad Branch Road NW, Washington, D.C. 20015, United States

ABSTRACT: The high-pressure behavior of H_2O ice at temperatures below 100 K has been investigated to 20 GPa by Raman spectroscopy. Between 10 and 80 K, high density amorphous (hda) ice formed from ice I_h undergoes a phase transition near 5 GPa to ice VII′ and a transition at 14 GPa to a different phase. At 14 GPa, a new low-frequency band appears at ∼150 cm^{-1} that steeply increases in frequency with pressure. The phase can be recovered to 0.1 MPa at temperatures below 80 K, and it transforms to low density amorphous ice (lda) upon heating. The phase is only present below 140 K and has spectral features that are identical to the phase formed from ice VIII at these pressures and temperatures. Similar changes have been observed in ice VII at these pressures but at room temperature. The results suggest structural changes having a common origin.

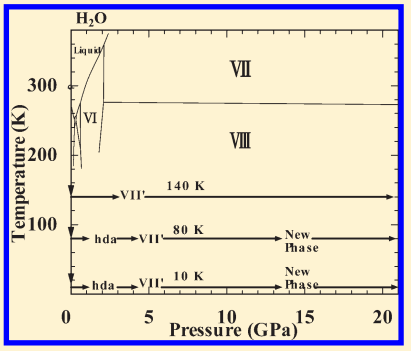

I. INTRODUCTION

The variety of forms of ice is one of the distinctive features of H_2O in condensed phase.[1−5] Transitions involving these phases can be induced by combinations of pressure and temperature, which give rise to a complex phase diagram of ice especially at low pressures and temperatures. Another notable feature of H_2O is its propensity to form metastable phases, including both amorphous and crystalline forms. Denser crystalline phases known as ice VII and ice VIII form above 2 GPa that can be described as interpenetrating network structures of ice I_c. Using in situ techniques, Hemley et al.[6] investigated the transformation of ice I_h to high-density amorphous (hda) ice and probed its stability and metastable transitions to other ices under various pressure and temperature conditions and paths. They found that when pressurized in the stability field of ice VIII, hda crystallizes into a phase with spectral features similar to ice VII (called ice VII′). Klotz et al.[7] later showed that by cooling ice VI below 95 K at 1.5 GPa and compressing it isothermally, metastable ice VII forms around 4 GPa through a metastable transition. A phase that appears to be closely related to ice VII′ can be recovered to ambient pressure at temperatures below 95 K. Song et al.[8] subsequently investigated the metastability of this form of ice VII as a function of pressure and temperature by infrared absorption spectroscopy; they showed that ice II can also transform to ice VII′, which they attributed to its mechanical instability upon compression below 150 K.

Subsequent synchrotron X-ray diffraction and Raman measurements at high pressure and low temperatures provided evidence for a structural change in ice VIII between 10 and 14 GPa.[9] On compression, the $\nu_{Tz}A_{1g} + \nu T_{x,y}E_g$ Raman lattice mode observed at 200−250 cm^{-1} disappears near 10 GPa and a new peak at ∼150 cm^{-1} appears indicative of a structural change that is complete by 14 GPa. Coincident with these changes in vibrational spectra, the unit cell axial ratio c/a obtained from X-ray diffraction shows anomalous changes at 10−14 GPa. This form of ice was tentatively identified as ice VIII′. Evidence for a structural change has also been found in ice VII at these pressures and room temperatures.[10] These pressure-induced effects in ices VII and VIII have implications for the behavior of ice at higher pressure, including the transition to ice X.[11,12]

Here we explore the properties and stability of ice VII′ up to 20 GPa by Raman spectroscopy at temperatures between 10 and 140 K. We find evidence for a structural transition in ice VII′ at ∼14 GPa. The phase can be quenched to 0.1 MPa at 80 K and transforms to low density amorphous ice (lda) upon heating. The phase formed from ice VII′ has spectral features that are similar to the phase produced from ice VIII at these conditions. The results suggest the formation of a common structure at these pressures that is independent of $P-T$ path and starting phase.

2. EXPERIMENTAL METHODS

Distilled and deionized water and pressure markers (ruby chips) were loaded in Mao-Bell-type diamond anvil cells (DACs) using stainless steel gaskets. The DACs were mounted in a liquid-nitrogen or -helium cryostat equipped with a spring-loaded lever arm system, which enables in situ pressure charges. Two resistive heaters and a diode sensor were directly attached to the DAC for controlling and monitoring the temperature of the sample during

Received: December 2, 2010
Revised: March 1, 2011
Published: March 22, 2011

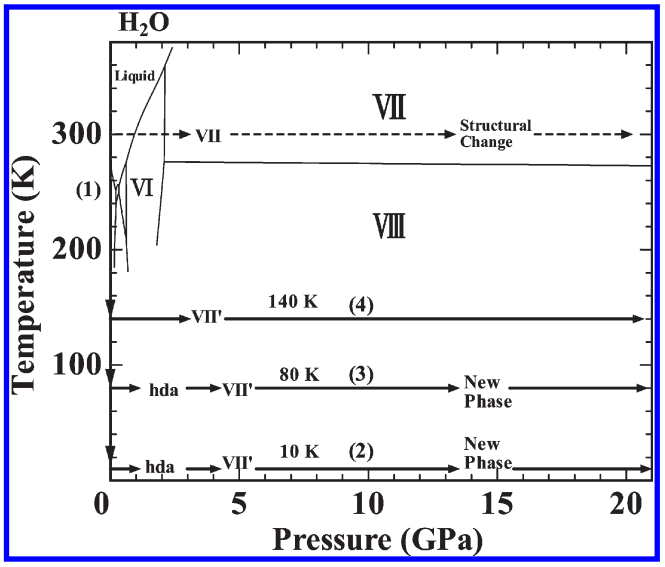

Figure 1. Schematic showing experimental paths performed in the present study on the equilibrium phase diagram of H_2O. The dashed line is from Somayazulu et al.[10]

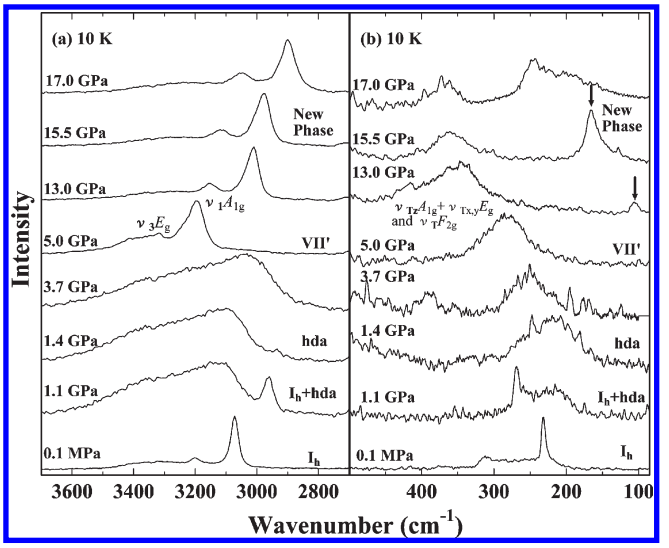

Figure 2. (a) In-situ Raman spectral changes at 10 K in the region of the OH stretching vibrations as a function of pressure [path 2]. (b) In-situ Raman spectral changes at 10 K in the region of the translational vibrations as a function of pressure [path 2]. Arrows show new bands appearing above ~14 GPa.

the measurements. The pressure was determined using the R_1 fluorescence technique.[13,14] Raman spectra under high pressure were collected by a single-grating ISA HR-460 spectrometer equipped with a charge-coupled device (CCD) detector. The 514.5 nm line of an argon-ion laser was typically used. Ice was compressed and data was collected at 10, 80, and 140 K as the sample was compressed to ~20 GPa.

3. RESULTS AND DISCUSSION

The experimental paths are shown schematically in Figure 1 superposed on the equilibrium phase diagram of H_2O. In all paths, ice I_h was the starting common phase obtained by cooling liquid water in the DAC (path 1). Subsequently, the sample was compressed to ~20 GPa while holding it at constant temperatures of 10, 80, and 140 K (paths 2, 3, and 4), respectively. Raman spectra were measured isothermally at 10, 80, and 140 K. We could follow the OH stretching vibrational mode of ice VII′ up to ~22 GPa, but above that point, the ν_1A_{1g} and ν_3E_g stretching modes overlap with the second-order Raman band of the diamond anvils.[15]

3.1. Raman Spectra at 10 K. Typical changes in the Raman spectra of ice on isothermal compression at 10 K are shown in Figure 2a and b for the OH-stretching and low-frequency regions, respectively. The hda phase was obtained by compressing ice I_h to 1.4 GPa. The spectrum at 1.1 GPa corresponds to the mixture of ice I_h and hda. On further compression, complete transformation was observed, followed by the transition to low-temperature ice VII′ at 4−5 GPa in agreement with ref 6. The formation of the ice VII′ phase is readily identified from the spectral profiles reported previously.[6,16] All of the fundamental Raman-active vibrations of normal ice VII at room temperature were reported by Pruzan et al.[17,18] In the OH stretching region, ice VII has three bands, ν_1A_{1g}, ν_3E_g, and ν_1B_{1g}; the ν_3E_g and ν_1B_{1g} modes are not well resolved (in comparison to ice VIII) probably due to the orientational disorder of the molecules. In the low-frequency (lattice mode) region, we observe a broad band at ~280 cm^{-1} that can be assigned to overlapping translational modes[18] of $\nu_{Tz}A_{1g} + \nu_{Tx,y}E_g$ and ν_TF_{2g}. Inspection of Figure 2 reveals significant spectral changes above 14 GPa. A new band around 110 cm^{-1} appears at 13 GPa whose frequency increases rapidly with pressure.

The conventional view has been that the orientations of molecules in ice VII are dynamically disordered, and all four proton positions around each oxygen atom are occupied. The dynamics of proton motion slows substantially with decreasing temperature and the protons become effectively frozen below 100 K. The width of the ν_1 stretching mode band in ice VII measured at room temperature exhibits a minimum around 13 GPa. Pruzan et al.[17] proposed that the pressure dependence of proton disorder separates into two regimes. Below 14 GPa, the orientational disorder occurs along the O−O directions; proton ordering first increases and then decreases with pressure. An alternative explanation[19] attributes these changes to modifications of the oxygen sublattice which in turn affect the compressional modes. Song et al.[8] reported measurements of the $P-T$ phase boundary between ice VII and ice VIII below 100 K by IR spectroscopy. The boundary at 30 GPa was found to be essentially insensitive to temperature over the measured range.

Keeping these features of the normal ice VII in mind, we offer a plausible explanation for the appearance of the new phase above 14 GPa in low-temperature ice VII′. We know that under pressure the O−H bond length does not increase significantly up to 30 GPa, while the hydrogen-bonded O−O distance decreases from 2.98 Å at 0.1 MPa to 2.54 Å at 30 GPa.[8,20] We assume that the orientational disorder in low-temperature ice VII′ is static and the dipole−dipole interaction is enhanced with increasing pressure. The extent of the frozen-in disorder in the system increases with increasing temperature, thereby modifying the dipolar interaction between the two ice I_c networks. We note that the $\nu_{Tz}A_{1g}$ mode involves the relative displacement of the two substructures along the axis. It is most likely that initially the intranetwork O···O distances are longer to allow for the interpenetration, but upon compression above 14 GPa steric effects and/or repulsion between molecules occur. We speculate that as a result of the compensation for these stresses

dx.doi.org/10.1021/jp111499x |J. Phys. Chem. B 2011, 115, 3756–3760

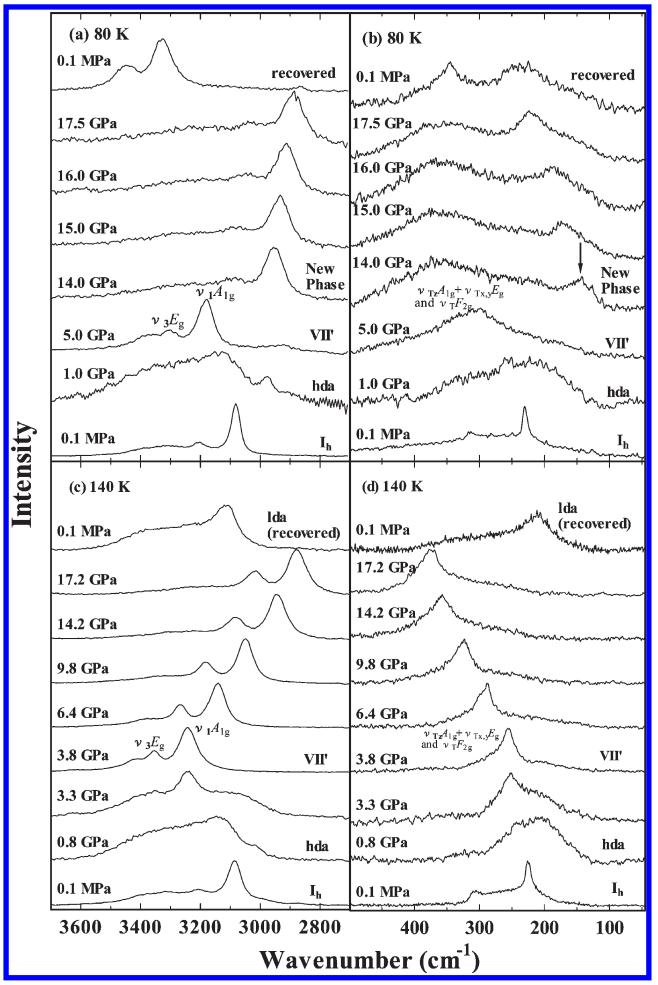

Figure 3. (a) In-situ Raman spectra at 80 K in the region of the OH stretching vibrations as a function of pressure [path 3]. (b) Spectra at 80 K in the region of the translational vibrations [path 3]. The arrow shows a new band appearing above ~14 GPa. (c) Spectra at 140 K in the region of the OH stretching vibrations [path 4]. (d) Spectra at 140 K in the region of the translational vibrations [path 4].

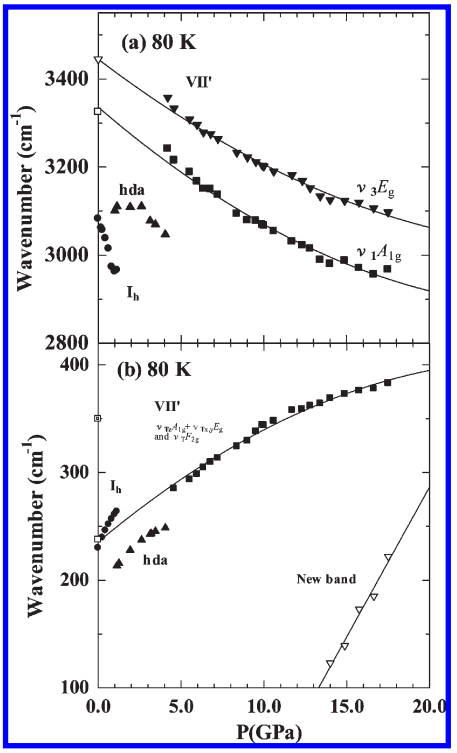

Figure 4. (a) Pressure dependence of the frequency of the OH stretching vibrational modes along path 3. The solid lines are fitted by a least-squares method. The open symbols represents the values for the retrieved state of ice VII′ at 0.1 MPa. (b) Pressure dependence of the frequency of the low-frequency region along isothermal path 3. The double square is the value for a band that appears in the recovered state. The solid lines are least-squares method-fits. The open symbols represent the values for the recovered state of ice VII′ at 0.1 MPa.

in the system coupled with the expectations that the molecular motions at low temperature (e.g. ~10 K) are slow, the new phase appears.

In this regard, it is interesting to note that Loubeyre et al.[21] reported evidence for spatially modulated (incommensurate) phases of normal ice VII with no distortion from the cubic structure between 2.2 and 25 GPa at room temperature. The modulated phases were reported to be intrinsic properties of ice VII that disappear in strained crystals or in polycrystalline ice. Similar phenomenon may be expected in the phases studied here due to the magnitudes of the competing dipolar interactions induced by applied pressure. Comparison between the structure of the phase observed here and modulated ice VII awaits detailed diffraction measurements produced by both paths.

3.2. Raman Spectra As a Function of Temperature. We carried out a series of isothermal compression experiments on ice I_h at temperatures above 10 K [at 80 K (path 3) and at 140 K (path 4) in Figure 1] to explore the stability region of the new phase appeared in low temperature ice VII′. We observe the same transformation sequence at 80 K at nearly identical pressures (Figure 3a and b). However, at the higher temperature of 140 K, it is clear that the new band in the lower frequency region is not observed at these pressures (Figure 3d).

To look into more closely, we present the pressure dependence of frequencies of the vibrational bands at 80 K in Figure 4. The results at 10 K are almost coincident with those at 80 K. The frequency of a new band increases rapidly with pressure. Extrapolation of the soft-mode feature to zero frequency gives an onset pressure for the transition at a pressure close to (but less than) 13 GPa. An intriguing observation is the appearance of a new Raman peak at 350 cm^{-1} on recovery of the new phase at 0.1 MPa and 80 K. We propose that an adaptive structure regarded as a locking-in of the modulation proposed for ice VII[10] may relax in a different way in the recovered phase. On the other hand, we note that the phase observed here directly transforms to lda by isothermal decompression to ambient pressure at 140 K (Figure 3c and d). The phase can be quenched to 0.1 MPa below 80 K and directly transforms to lda above 120 K upon heating.

In-situ observations of the transformations of ice VII′ as functions of pressure and temperature revealed an additional transformation above 150 K.[6] Upon isobaric heating (e.g., 5.5 GPa) from 77 K to above 150 K, pressurizing ice VII′ results in ice VIII, which is the stable phase in this $P-T$ region.[6] In contrast, isothermal compression near 150 K of hda from ice I_h transforms to ice VIII at 2.4 GPa. Moreover, Klotz et al.[22] observed the recrystallization behavior of hda in the pressure range 0.3−0.9 GPa by in-situ neutron diffraction. They provided information that at 175 K and 0.4−0.7 GPa hda transforms to mainly phases

dx.doi.org/10.1021/jp111499x |J. Phys. Chem. B 2011, 115, 3756–3760

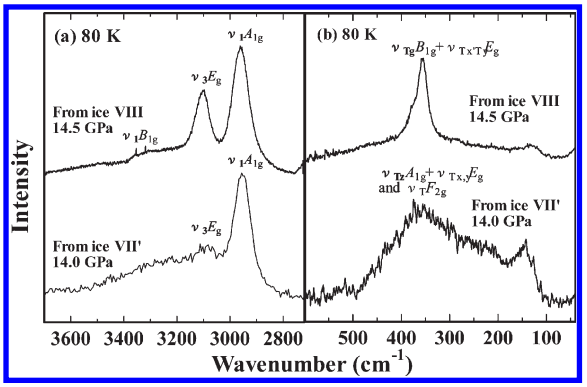

Figure 5. (a) Comparison of the Raman spectra of ice VII′ produced from hda and ice VIII′[9] from ice VIII in the OH stretching region. (b) Comparison of the spectra of ice VII′ and ice VIII′[9] in the low-frequency region.

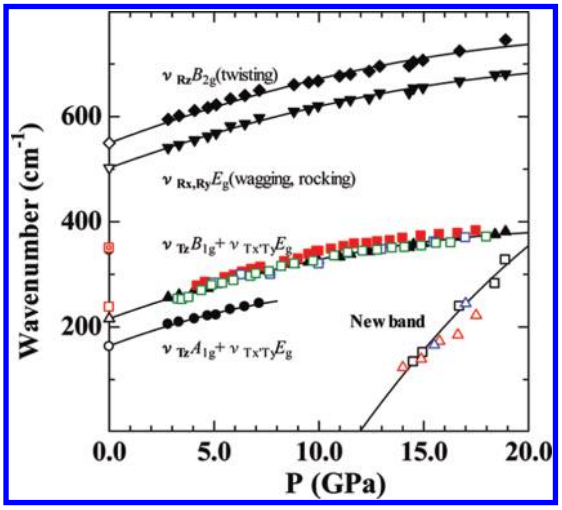

Figure 6. Comparison of the pressure dependences of the frequencies in the low-frequency region along different isothermal paths. The black symbols correspond results for ice VIII at 80 K.[9] The data for ice VII′ are given by the blue (10 K), red (80 K), and green (140 K) symbols. The red double squares show the shift in the soft mode feature that appears in the recovered phase studied here at 80 K and matches that of recovered ice VIII′.[9] The open red squares represent the retrieved state of the phase recovered under ambient pressure at 80 K. The solid lines represent least-squares fits. The shifts for the $\nu_{Tz}B_{1g} + \nu T_{x,y}E_g$ lattice mode of ice VIII and the overlapping bands of ice VII′ can be fitted by the same curve.

IV, V, and XII, but at 1−1.2 GPa, it forms a mixture of ice VI and XII. Upon compression at 100 K, hda crystallizes to form ice VII′. The phase produced here from ice VII′ via hda is stabilized below 140 K, and the transformation to it is kinetically controlled. Moreover, as stated in the introduction, X-ray measurements carried out on compression of ice VII at 300 K revealed the existence of structural changes near 14 GPa.[10] The transition can be interpreted as ferroelastic, i.e., arising from spontaneous strain in which the cubic symmetry in ice VII breaks down at this pressure. Taken together, we suspect that a nearly temperature-independent transition to the same structure (or related structures) is observed in all of these experiments.

3.3. Raman Spectra of Low Temperature Phases. The $P-T$ range of the present study is identical to our previous work which led to the observation of ice VIII′. However, the $P-T$ paths for reaching the phases are different. As mentioned above, in the study of ice VIII at 80 K, we observed the disappearance of the ∼208 cm^{-1} peak (the $\nu_{Tz}A_{1g} + \nu T_{x,y}E_g$ lattice mode) and the appearance of a new band at 150 cm^{-1} that exhibited a strong positive pressure shift. Figure 5 compares spectra for the different sets of results at 80 K and ∼14 GPa. The spectral profiles are similar but have different features in the low-frequency region. Detailed comparison between the transitions observed in ice VIII and ice VII′ observed in this study provides compelling evidence for the stabilization of a similar structure. Figure 6 shows a comparison of the available data.[9] The results for ice VII′ are close to those obtained for ice VIII at 80 K. The "soft mode" on decompression that appears above 14 GPa reported in ice VIII′ is also clearly seen. The results indicate that the same spectral features accompany the transition following different $P-T$ paths. The identification of this structure, as well as the nature of the possible order−disorder, requires detailed X-ray and neutron diffraction measurements.

4. CONCLUSIONS

The present study provides surprising new information about the phase behavior of ice at low temperature and modest pressures up to 20 GPa. Similar to our previous study of ice VIII, signatures of a structural modification near 14 GPa are evident from changes in Raman spectra obtained from compression of hda ice produced from ice I_h. The close similarity to Raman features found in ice VII at these pressures and room temperature indicate that similar structural features are stabilized at these densities, independent of $P-T$ paths. The connections between these transitions and the nature of the structural motif and associated order−disorder remain to be fully explored. The study provides baseline Raman data for understanding the evolution of the structure of ice at higher pressures. The results could have implications for planetary science where metastable transitions of H_2O are expected and should stimulate additional theoretical studies of the system as functions of pressure and temperature.

AUTHOR INFORMATION

Corresponding Author

*E-mail: muki@nda.ac.jp. Tel.: +81-46-841-3810 (ext 3583). Fax: +81-46-844-5901.

ACKNOWLEDGMENT

We are grateful to M. Guthrie and S. Gramsch for comments in the manuscript. This work was supported by NASA-PG&G, NASA-NAI, NSF-DMR, NSF-EAR, and DOE (NNSA) through CDAC.

REFERENCES

(1) Whalley, E. In *The Hydrogen Bond*; Schuster, P., Zundel, G., Sandorfy, C., Eds.; North-Holland: Amsterdam, 1976.
(2) Bridgman, P. W. *J. Chem. Phys.* **1937**, *5*, 964.
(3) Kamb, B. *Trans. Am. Chrystallog. Assoc.* **1969**, *5*, 61.
(4) Petrenko, V. F.; Whitworth, R. W. *Physics of Ice*; Oxford University Press: New York, 1999.
(5) Dunaeva, A. N.; Antsyshkin, D. V.; Kuskov, O. L. *Solar Syst. Res.* **2010**, *44*, 202.
(6) Hemley, R. J.; Chen, L. C.; Mao, H. K. *Nature* **1989**, *338*, 638.

(7) Klotz, S.; Besson, J. M.; Hamel, G.; Nelmes, R. J.; Loveday, J. S.; Marshall, W. G. *Nature* **1999**, *398*, 681.
(8) Song, M.; Yamawaki, H.; Fujihisa, H.; Sakashita, M.; Aoki, K. *Phys. Rev. B* **2003**, *68*, 024108.
(9) Yoshimura, Y.; Stewart, S. T.; Somayazulu, M.; Mao, H. K.; Hemley, R. J. *J. Chem. Phys.* **2006**, *124*, 024502.
(10) Somayazulu, M.; Shu, J.; Zha, C. S.; Goncharov, A. F.; Tschauner, O.; Mao, H. K.; Hemley, R. J. *J. Chem. Phys.* **2008**, *128*, 064510.
(11) Goncharov, A. F.; Struzhkin, V. V.; Somayazulu, M.; Hemley, R. J.; Mao, H. K. *Science* **1996**, *273*, 218.
(12) Aoki, K.; Yamawaki, H.; Sakashita, M.; Fujihisa, H. *Phys. Rev. B* **1996**, *54*, 15673.
(13) Chervin, J. C.; Canny, B.; Guthier, M.; Pruzan, P. *Rev. Sci. Instrum.* **1993**, *64*, 203.
(14) (a) Mao, H. K.; Bell, B. M.; Shaner, J. W.; Steinberg, D. J. *J. Appl. Phys.* **1978**, *49*, 3276. (b) Mao, H. K.; Xu, J.; Bell, P. M. *J. Geophys. Res.* **1986**, *91*, 4673.
(15) Hirsch, K. R.; Holzapfel, W. B. *J. Chem. Phys.* **1986**, *84*, 2771.
(16) Yoshimura, Y.; Mao, H. K.; Hemley, R. J. *Chem. Phys. Lett.* **2006**, *420*, 503.
(17) Pruzan, P.; Chervin, J. C.; Guthier, M. *Europhys. Lett.* **1990**, *13*, 81.
(18) Pruzan, P.; Chervin, J. C.; Wolanin, E.; Canny, B.; Guthier, M.; Hanfland, M. *J. Raman Spectrosc.* **2003**, *34*, 591.
(19) Besson, J. M.; Kobayashi, M.; Nakai, T.; Endo, S.; Pruzan, P. *Phys. Rev. B* **1997**, *55*, 11191.
(20) Nelmes, R. J.; Loveday, J. S.; Wilson, R. M.; Besson, J. M.; Pruzan, Ph.; Klotz, S.; Hamel, G.; Hull, S. *Phys. Rev. Lett.* **1993**, *71*, 1192.
(21) Loubeyre, P.; Letoullec, R.; Wolanin, E.; Hanfland, M.; Hausermann, D. *Nature* **1999**, *397*, 503.
(22) Klotz, S.; Hamel, G.; Loveday, J. S.; Nelmes, R. J.; Guthrie, M. *Z. Kristallogr.* **2003**, *218*, 117.